Available online at www.sciencedirect.com
ScienceDirect
Materials Letters 61 (2007) 448–451
materials letters
www.elsevier.com/locate/matlet

Adhesive forces significantly affect elastic modulus determination of soft polymeric materials in nanoindentation

Shikha Gupta [a,c], Fernando Carrillo [b], Cheng Li [c], Lisa Pruitt [d], Christian Puttlitz [e,*]

[a] Medical Polymers and Biomaterials Group, Department of Applied Science and Technology, University of California, Berkeley, USA
[b] Department of Chemical Engineering, EUETIT, Polytechnic University of Catalonia, Terrassa, Barcelona, Spain
[c] UCB/UCSF Joint Program in Bioengineering, University of California, Berkeley, USA
[d] Department of Mechanical Engineering, University of California, Berkeley, USA
[e] Department of Mechanical Engineering, Colorado State University, Fort Collins, CO 80523-1374, USA

Received 7 September 2005; accepted 20 April 2006
Available online 11 May 2006

Abstract

The present study investigated the effects of adhesion on the elastic modulus determined from nanoindentation curves for soft polydimethylsiloxane (PDMS) elastomers with five different crosslink concentrations. Indentation load-displacement curves were obtained for samples of all concentrations at four different peak loads. All load–displacement curves were nearly linear, resulting in load independent contact stiffnesses ($p<0.003$) for the range of loads tested. As a result, elastic modulus calculated from nanoindentation curves with the Hertz contact model exhibited significant differences ($p<0.004$) both at different peak loads for a single PDMS concentration and between different PDMS concentrations at a single peak load ($p<0.001$). The differences for different peak loads were attributed to the presence of substantial adhesive forces at the tip–sample interface. By taking these adhesive interactions into account with the Johnson, Kendall, Roberts (JKR) contact model, the differences in elastic modulus at different peak loads could be reconciled. Significant differences ($p<0.001$) in moduli between different PDMS concentrations were still present. The results highlight the importance of considering adhesive forces in nanoindentation analyses of low modulus polymeric materials.

1. Introduction

As compliant elastomeric polymers find greater use in microfabricated devices [1,2], nanocomposites [3], and tissue engineering scaffolds [4,5], suitable techniques for determining the mechanical properties of these materials at the nanoscale must be devised. While bulk mechanical testing techniques, such as uniaxial tension, unconfined compression and rheometry can be readily used to characterize bulk homogeneous specimens, the presence of small testing volumes and material heterogeneities confounds the use of these techniques in the above applications. With its ability to map localized mechanical properties on a submicron scale, nanoindentation has effectively been utilized to characterize many different materials, including metallic and piezoelectric films [6,7], polymeric coatings [8], and even mineralized tissues such as bone and teeth [9,10]. Since nanoindentation theory and instrumentation were initially developed for hard, elasto-plastic materials however [11–13], studies with soft polymeric materials have been very limited [14,15]. Thus, nanoindentation of these compliant materials still requires further validation and suitable modification to obtain quantitatively accurate and reproducible results.

Traditional indentation analyses are based on the Hertz contact model [16], applicable for ideal elastic materials experiencing infinitesimal deformations. According to the Hertz model, for indentation of a flat smooth substrate by a rigid, spherical indenter, the elastic modulus of the substrate can be obtained from indentation load–displacement curves as follows:

$$E_H = \sqrt{\frac{S^3(1-\nu^2)^2}{6RP}} \quad (1)$$

where E_H is the elastic modulus of the substrate, ν is the Poisson's ratio of the substrate, R is the nominal radius of curvature of the indenter tip, P is the applied load, and S is the

* Corresponding author. Tel.: +1 970 491 0956.
E-mail address: puttlitz@engr.colostate.edu (C. Puttlitz).

0167-577X/$ - see front matter © 2006 Elsevier B.V. All rights reserved.
doi:10.1016/j.matlet.2006.04.078

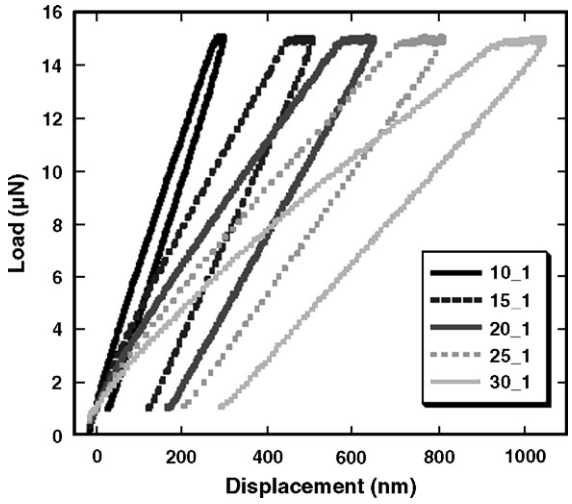

Fig. 1. Load vs. displacement curves for different PDMS crosslink concentrations at 15 μN applied load.

material stiffness ($S = dP/dh$) evaluated at P. The classic Hertz's model is a hard contact model that does not take adhesive interactions into account. The Johnson, Kendall, Roberts (JKR) model, which accounts for interfacial forces outside the Hertzian contact area, is the most applicable adhesion model for compliant materials indented with spherical probes with a large radius of curvature [17–19]. According to the JKR model:

$$E_{\mathrm{JKR}} = \sqrt{\frac{S^3(1-\nu_s^2)^2}{6R}\cdot\left[\left(\frac{2}{3\sqrt{1+\frac{P}{F_{\mathrm{po}}}}}+1\right)^3\frac{1}{P+2F_{\mathrm{po}}+2F_{\mathrm{po}}\sqrt{\left(1+\frac{P}{F_{\mathrm{po}}}\right)}}\right]} \quad (2)$$

where F_{po} is the adhesive pull-off force at the tip–sample interface. Since adhesive interactions may play a significant role in nanoscale contact mechanics, the following study further elucidates the effects of adhesion forces on the elastic modulus determination of soft (E_{H} less than 5 MPa) polydimethylsiloxane (PDMS) elastomers by nanoindentation [19].

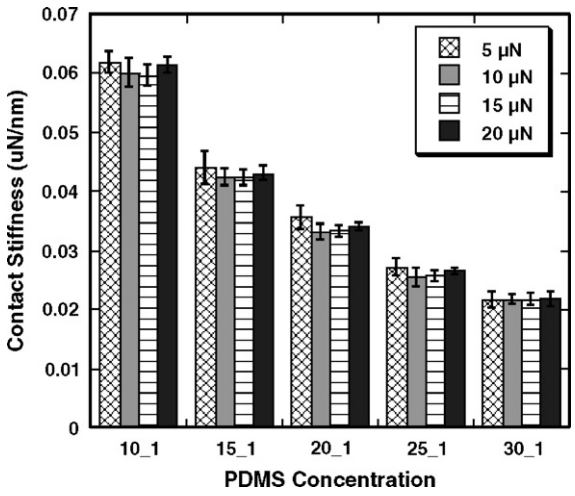

Fig. 2. Unloading stiffness of different PDMS concentrations (10_1 to 30_1) at 5, 10, 15, and 20 μN peaks' applied load. Linearity of the load–displacement curves leads to stiffness values that are nearly independent of the applied load ($p > 0.05$) for each concentration, though significant differences ($p < 0.001$) exist between different PDMS concentrations. Samples with the highest ratio of base to crosslinking agent (25_1 and 30_1) are the most compliant.

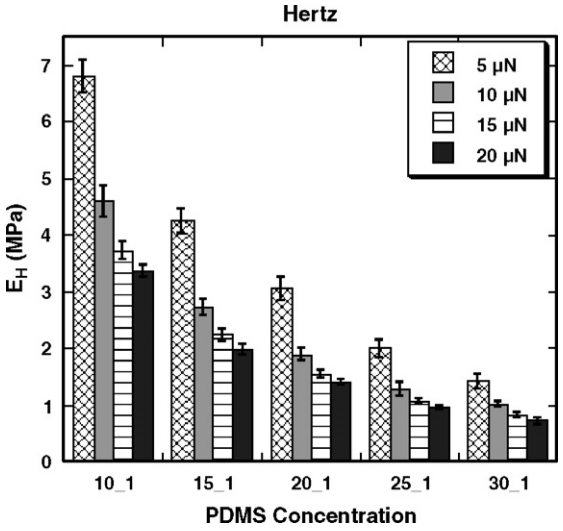

Fig. 3. Elastic modulus calculated from the Hertz model (Eq. (1)). Significant differences in E_{H} are observed both for different applied loads for a single PMDS concentration ($p < 0.0028$) and between different PDMS concentrations for a single applied load ($p < 0.0014$).

2. Materials and methods

Details of the PDMS sample preparation method have been published elsewhere [19]. In brief, 15 samples were prepared by mixing five different ratios (10:1, 15:1, 20:1, 25:1 and 30:1) of a siloxane monomer with a crosslinking agent (Sylgard Elastomer 184, Dow Corning Corporation, Midland, MI, USA). Solutions were mixed and poured in containers with a glass bottom surface.

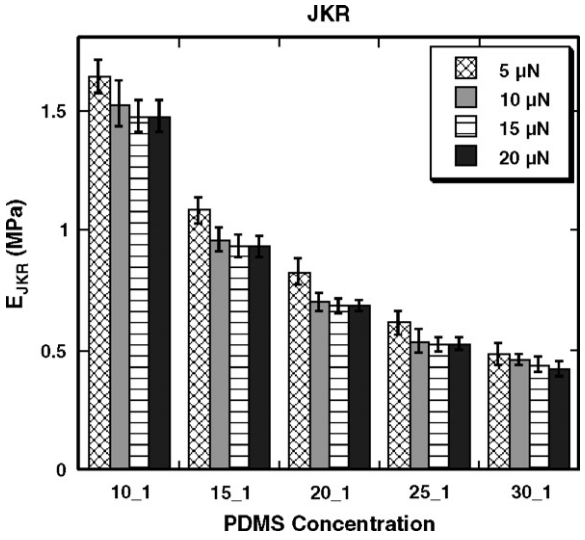

Fig. 4. Elastic modulus calculated from the JKR model (Eq. (2)). Significant differences in E_{JKR} are observed between different PDMS concentrations for a single applied load ($p < 0.0014$). There are no significant differences in E_{JKR} for different applied loads for the 10_1, 15_1, and 30_1 PDMS concentrations. For 20_1 and 25_1, there are significant differences between E_{JKR} for 5 μN and 10 μN peak loads only.

Samples were cured for 2 weeks at room temperature, cut, and subsequently glued to metal platens for nanoindentation testing.

Nanoindentation measurements were performed using a Hysitron TriboIndenter (Hysitron Inc., Minneapolis, MN) with closed loop feedback in load-controlled mode. Bearing in mind small deformation constraints, 5, 10, 15 and 20 μN peak loads were applied to each sample at room temperature using a 100 μm radius of curvature diamond conospherical tip. A trapezoidal loading profile was selected; once the tip was brought into contact with the sample, the load was applied at a rate of 1 μN/s, held for 20 s at the maximum load to permit viscoelastic dissipation, and subsequently withdrawn at a rate of 1 μN/s. Load and displacement were recorded simultaneously during indentation. Multiple indents (10–12) were performed at each of the four loads for all five PDMS crosslink concentrations (220 indents total). Indentation stiffness ($S = dP/dh$) was evaluated at the maximum load and depth from the initial unloading portion of the load–displacement (L–D) curve. Pull-off forces (F_{po}) between the diamond conospherical tip and PDMS substrates, as measured by Carrillo et al. [19], were then used to calculate elastic moduli from load displacement curves using both the Hertz and JKR models (Eqs. (1) and (2)). Statistical analyses were performed using a one-way analysis of variance (ANOVA) with Fisher's least significant difference PLSD post hoc test for multiple comparison (Statview, version 5.0, SAS Institute Inc., NC, USA). In all cases, p-values less than 0.05 were considered statistically significant.

3. Results

Fig. 1 shows typical L–D curves for the different PDMS concentrations at 15 μN applied load, with similar trends observed for the other loads. The L–D curves for all PDMS concentrations are nearly linear for the range of loads tested. Thus, there are no significant differences ($p > 0.05$) in the unloading indentation stiffness at different loads for a single PDMS concentration (Fig. 2). However, stiffness values between different PDMS concentrations for the same applied load are significantly different ($p < 0.05$). As expected, samples with higher monomer to crosslinker ratios (25_1, 30_1) are more compliant (Fig. 2).

The Hertz elastic moduli (E_H) calculated from the stiffness values (Fig. 3) exhibit substantial variations with both applied load and PDMS concentration. For all samples there are significant differences ($p < 0.003$) in E_H between all four applied loads for a single PDMS concentration. For a given applied load, there is also a significant difference ($p < 0.001$) in E_H with PDMS crosslink concentration.

In order to elucidate the effect of adhesive forces on elastic modulus determination, the JKR model (Eq. (2)) was used. Previously [19] calculated values for F_{po} varied from 93.1 ± 6.8 μN (for PDMS 10-1) to 43.6 ± 3.6 μN (for PDMS 30-1). Taking these adhesive forces into account, the elastic moduli calculated according to the JKR model (E_{JKR}) are nearly equivalent for different applied loads for each PDMS concentration (Fig. 4), though the values are less than half the magnitude of the corresponding E_H. The significant differences in modulus with PDMS crosslink concentration are maintained for E_{JKR}.

4. Discussion

PDMS is known to exhibit nearly ideal elastic behavior under finite strain conditions with minimal viscoelastic effects (tan $\delta < 0.01$). Hence, the elastic modulus should be constant and consistent for a range of nanoindentation loading conditions. According to the Hertz's model, for a linear elastic material, a constant value for E_H is obtained only when the indentation stiffness is proportional to the applied load as follows: $S \propto P^{1/3}$. In the present experiments, S is independent of P for 5 μN ≤ P ≤ 20 μN. According to Eq. (1), E_H is then proportional to $P^{-1/2}$, rendering the calculated E_H value a stress-dependent quantity.

For the JKR model (Eq. (2)), E_{JKR} is a non-linear function of P and F_{po}. For a constant indentation stiffness, as obtained in the preceding experiments, $E_{JKR} \propto f(P, F_{po}, P/F_{po})^{-1/2}$. For the PMDS concentrations tested, F_{po} may be anywhere from 2 to 20 times the applied load P. In this case, $E_{JKR} = (KF_{po})^{-1/2}$, where K is approximately constant. Thus, E_{JKR} is also nearly independent of P, with the absolute value determined experimentally from S and F_{po}. In fact, the presence of substantial adhesive forces is also what leads to S values that are independent of P for the PDMS samples. The indentation stiffness measured from L–D curves is dependent upon the total load ($P + F_{po}$) experienced by the material. For linear elastic materials with adhesive interactions, the indentation stiffness is supposed to be a non-linear function of both components (P, F_{po}) of the total load. If F_{po} dominates the total load, the stiffness do not change significantly with the increasing applied load (P), leading to nearly linear L–D curves.

The preceding work demonstrates that including adhesive forces in the analysis of the nanoindentation data elucidates the apparent linearity of the L–D curves and reconciles the differences in E_H observed at the different applied loads. This data unequivocally shows that consideration of the adhesion energy at the tip–sample interface is requisite for determining accurate elastic moduli of PDMS samples and other soft, elastomeric materials from nanoindentation experiments.

References

[1] S.M. Mitrovski, R.G. Nuzzo, An electrochemically driven poly(dimethylsiloxane) microfluidic actuator: oxygen sensing and programmable flows and pH gradients, Lab Chip 5 (6) (2005) 634–645.
[2] M. Mendoza, A. Carrillo, A. Marquez, New distributed optical sensor for detection and localization of liquid hydrocarbons — part II: optimization of the elastomer performance, Sens. Actuators, A, Phys. 111 (2–3) (2004) 154–165.
[3] G.J. van Maanen, S.L. Seelye, M.D. Capracotta, S.A. White, R.R. Bukovnik, J. Hartmann, J.D. Martin, R.J. Spontak, Property and morphology development in nanocomposite thermoplastic elastomer gels, Langmuir 21 (7) (2005) 3106–3115.
[4] J.J. Stankus, J.J. Guan, W.R. Wagner, Fabrication of biodegradable elastomeric scaffolds with sub-micron morphologies, J. Biomed. Mater. Res. Part A 70A (4) (2004) 603–614.
[5] T. Matsuda, M. Ihara, H. Inoguchi, K. Kwon, K. Takamizawa, S. Kidoaki, Mechano-active scaffold design of small-diameter artificial graft made of electrospun segmented polyurethane fabrics, J. Biomed. Mater. Res. Part A 73A (1) (2005) 125–131.
[6] Y. Zhou, C.S. Yang, J.A. Chen, G.F. Ding, W. Ding, L. Wang, M.J. Wang, Y.M. Zhang, T.H. Zhang, Measurement of Young's modulus and residual stress of copper film electroplated on silicon wafer, Thin Solid Films 460 (1–2) (2004) 175–180.
[7] P. Delobelle, True Young modulus of Pb(Zr,Ti)O-3 films measured by nanoindentation, Appl. Phys. Lett. 85 (22) (2004) 5185.

[8] X.H. Gu, T. Nguyen, L.P. Sung, M.R. VanLandingham, M.J. Fasolka, J.W. Martin, Y.C. Jean, D. Nguyen, N.K Chang, T.Y. Wu, Advanced techniques for nanocharacterization of polymeric coating surfaces, Jct Res. 1 (3) (2004) 191–200.
[9] J.Y. Rho, J.D. Currey, P. Zioupos, G.M. Pharr, The anisotropic Young's modulus of equine secondary osteones and interstitial bone determined by nanoindentation, J. Exp. Biol. 204 (2001) 1775–1781.
[10] S. Habelitz, S.J. Marshall, G.W. Marshall, M. Balooch, Mechanical properties of human dental enamel on the nanometer scale, Arch. Oral Biol. 46 (2001) 173.
[11] I.N. Sneddon, The relation between load and penetration in the axisymmetric Boussinesq problem for a punch of arbitrary profile, Int. J. Eng. Sci. 3 (1956) 47–56.
[12] M.F. Doerner, W.D. Nix, A method or interpreting the data from depth-sensing indentation instruments, J. Mater. Res. 1 (1986) 601.
[13] W.C. Oliver, G.M. Pharr, An improved technique for determining hardness and elastic modulus using load and displacement sensing indentation experiments, J. Mater. Res. 7 (1992) 1564–1583.
[14] J.C. Lötters, W. Olthuis, P.H. Veltink, P. Bergveld, The mechanical properties of the rubber elastic polymer polydimethylsiloxane for sensor applications, J. Micromech. Microeng. 7 (1997) 145–147.
[15] W.H. Xu, Z.Y. Xiao, T.Y. Zhang, Mechanical properties of silicone elastomer on temperature in biomaterial application, Mater. Lett. 59 (17) (2005) 2153–2155.
[16] H. Hertz, On the contact of elastic solids, J. Reine Angew. Math. 92 (1881) 156–171.
[17] K.L. Johnson, Contact Mechanics, Cambridge University Press, Cambridge, England, 1987.
[18] K.L. Johnson, K. Kendall, A.D. Roberts, Surface energy and the contact of elastic solids, Proc. R. Soc. Lond. A324 (1971) 301–313.
[19] F. Carrillo, S. Gupta, M. Balooch, L.A. Pruitt, S.J. Marshall, G.W. Marshall, C.M. Puttlitz, Nanoindentation of PDMS elastomers: effect of crosslinking, work of adhesion and fluid environment on elastic modulus, J. Mater. Res. 20 (10) (2005) 2820–2830.